Aligned ZnO Nanorod Arrays Grown Directly on Zinc Foils and Zinc Spheres by a Low-Temperature Oxidization Method

Zhanjun Gu,[†,‡] M. Parans Paranthaman,[§] Jun Xu,[§] and Zheng Wei Pan*[,†,‡]

[†]Faculty of Engineering and, [‡]Department of Physics and Astronomy, University of Georgia, Athens, Georgia 30602, and [§]Chemical Sciences Division, Oak Ridge National Laboratory, Oak Ridge, Tennessee 37831

ABSTRACT Vertically aligned, dense ZnO nanorod arrays were grown directly on zinc foils by a catalyst-free, low-temperature (450−500 °C) oxidization method. The zinc foils remain conductive even after the growth of ZnO nanorods on its surface. The success of this synthesis largely relies on the level of control over oxygen introduction. By replacing zinc foils with zinc microspheres, unique and sophisticated urchin-like ZnO nanorod assemblies can be readily obtained.

KEYWORDS: nanorod array · oxidization · ZnO · zinc foil · zinc microsphere

Zinc oxide (ZnO) is recognized as one of the most important photonic materials for applications in the blue−ultraviolet region owing to its direct wide bandgap (~3.37 eV) and large excitation binding energy (60 meV at room temperature).[1−4] Stimulated by the recent discovery of beltlike morphology[5] and the realization of room-temperature UV lasing from ZnO nanowires,[6] ZnO nanostructures in the form of nanorods, nanowires, and nanobelts have attracted a great deal of attention from the research community. Especially, substantial effort has been devoted to the fabrication of vertically aligned ZnO nanowire arrays because these arrays demonstrated superior optical and field emission properties that make them promising candidates for applications in UV lasers,[6] light-emitting diodes (LED),[7] solar cells,[8] and field emission displays.[9]

To fabricate vertically aligned ZnO nanorod arrays, three main techniques were usually used so far. The first technique is based on the well-known vapor−liquid−solid (VLS) growth mechanism,[10] in which gold nanoparticles were used as the catalyst to direct the nanowire growth, *a*-plane sapphire which has perfect lattice matchup with ZnO *c* plane was used as the growth substrates, and the growth was conducted at relatively high temperatures of 850−1000 °C.[6,11,12]

The second technique is metal−organic chemical vapor deposition (MOCVD), in which metal−organic zinc precursor (diethyl zinc, Et_2Zn) was used as the zinc source and aligned ZnO nanowires were epitaxially grown on sapphire

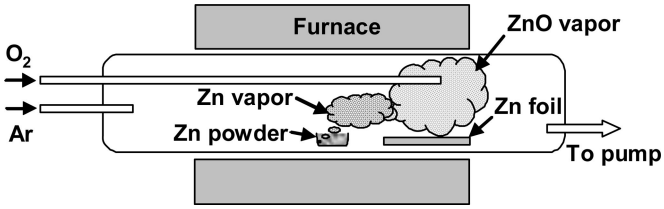

Figure 1. Schematic diagram of the experimental setup.

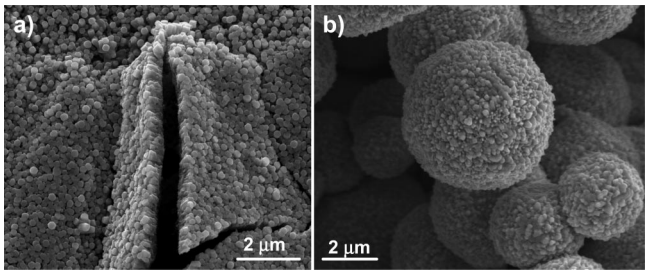

Figure 2. SEM images of ZnO nanopillars formed on (a) zinc foil and (b) zinc microsphere surfaces at the early growth stage, which act as the seeds for subsequent ZnO nanorod growth. The broken nanopillars film in panel A shows the cross section and thickness of the film.

*Address correspondence to panz@uga.edu.

Received for review November 11, 2008 and accepted January 01, 2009.

Published online January 13, 2009.
10.1021/nn800759y CCC: $40.75

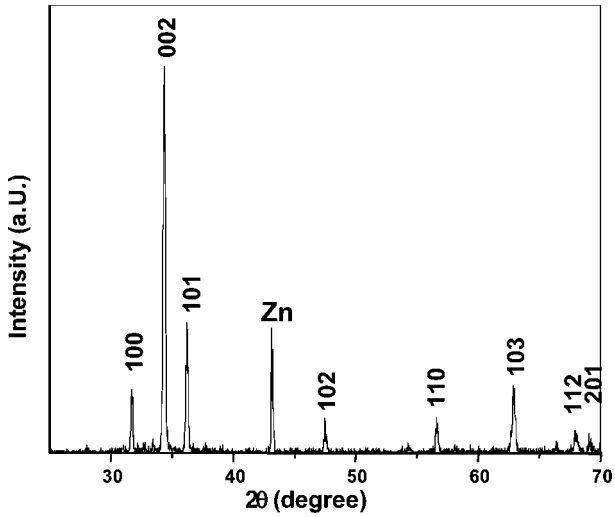

Figure 3. XRD pattern recorded from ZnO nanorod arrays grown on zinc foil.

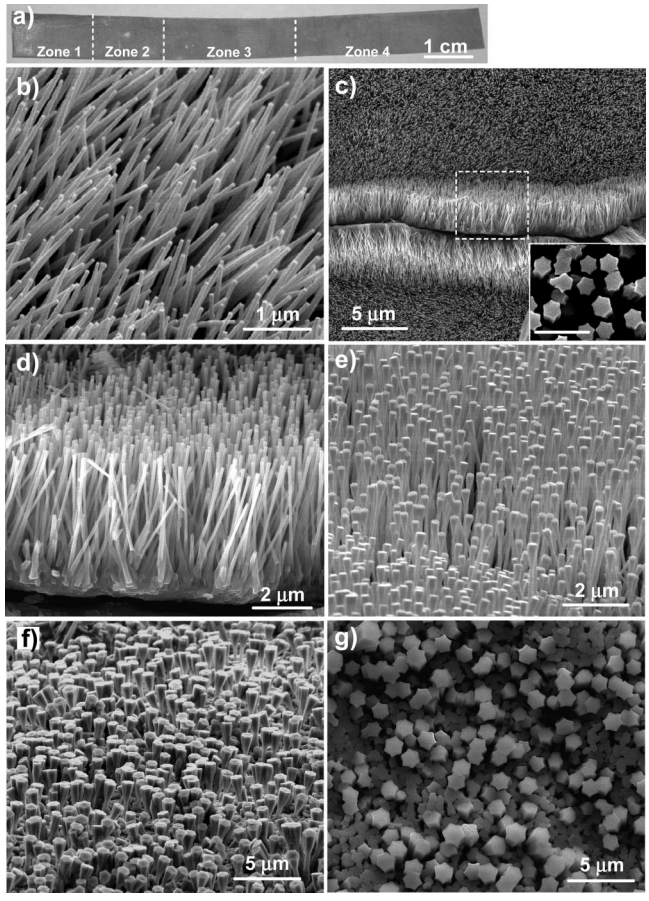

Figure 4. Vertically aligned ZnO nanorod arrays grown on zinc foils. (a) Digital image of a zinc foil (10 cm × 1 cm) after growth. On the basis of the morphologies and sizes of the nanorods, four growth zones were divided and labeled. (b) SEM image of a ZnO nanoneedle array grown in zone 1. (c) A broken ZnO nanorod array formed in zone 2. The inset is the top view of the nanorods showing hexagonal top surface. Scale bar, 1 μm. (d) An enlarged image of the box area in panel c, showing that the nanorods are grown vertically from a thin film of ZnO nanocrystals. (e) Side view of a ZnO nanonail array grown in zone 3 showing nail-like nanorods with increased diameter from the bottom to the top. (f) Side view and (g) top view of ZnO micronail arrays formed in zone 4.

substrates (or silicon wafers) at 400−500 °C in a low-pressure MOCVD system.[13−15] The third technique is based on solution method, in which ZnO nanocrystals (5−10 nm in diameter) were coated on a substrate (e.g., silicon wafer) to act as the seeds followed by hydrothermal ZnO growth in an aqueous solution of zinc nitrate hydrate at 90 °C.[16−19] The solution process is favored for its low cost and the ease of scale-up (arrays on four-inch silicon wafer and two-inch plastic substrates were reported[17]) but suffers from the low crystalline quality compared with the VLS- and MOCVD-grown nanowires. In addition, some electrical and optical applications of the above-mentioned ZnO nanowires remain constrained by the expensive and/or nonconducting substrates (such as sapphire).

In this paper, we report the controlled growth of vertically aligned ZnO nanorod arrays on metal zinc foils (10 cm long by 1 cm wide) by a catalyst-free, low-temperature (450−500 °C) oxidization method. More amazingly, by substituting the flat zinc foils with highly curved zinc microspheres, sophisticated urchin-like ZnO nanorod superstructures, such as ZnO nanorod balls/bowls whose surfaces were covered with dense, uniform ZnO nanorods, can be readily obtained.

RESULTS AND DISCUSSION

The growth was conducted inside a tube furnace system (Figure 1). Zinc powder was used as the source material and zinc foils (or zinc microspheres) were used as the growth substrates. To ensure the success of the synthesis, the introduction of oxygen needs to be carefully controlled. The issues related to oxygen introduction include (i) the position of the oxygen tube, (ii) the oxygen flow rate, and (iii) the time when the oxygen is introduced, which can be summarized as follows.

First, the outlet of the oxygen tube should be positioned downstream of the source zinc powder but right above the middle of the zinc foil. This avoids the oxidization of zinc powder, while generating an efficient, wide oxidizing region over the zinc foil to facilitate the ZnO nanorod growth.

Second, the oxygen gas flow rate needs to be controlled below 5 sccm (standard cubic centimeter per minute). If the oxygen flow rate is too high, the concentration of reactant species in the vapor will be so high that a thick layer of byproduct (such as random ZnO nanorods, ZnO tetrapods,[20] or ZnO nanocombs[21,22]) will be deposited on the surface of the nanorod arrays. The optimum oxygen flow rates were found to be in the range of 3−5 sccm.

Third, the oxygen gas needs to be introduced as soon as the furnace temperature reaches 600 °C. At this temperature the zinc powder located at the furnace center can be efficiently evaporated to feed the ZnO nanorod growth. Because of the temperature gradient of the furnace, the temperature in the growth region was measured to be about 450−500 °C, at which

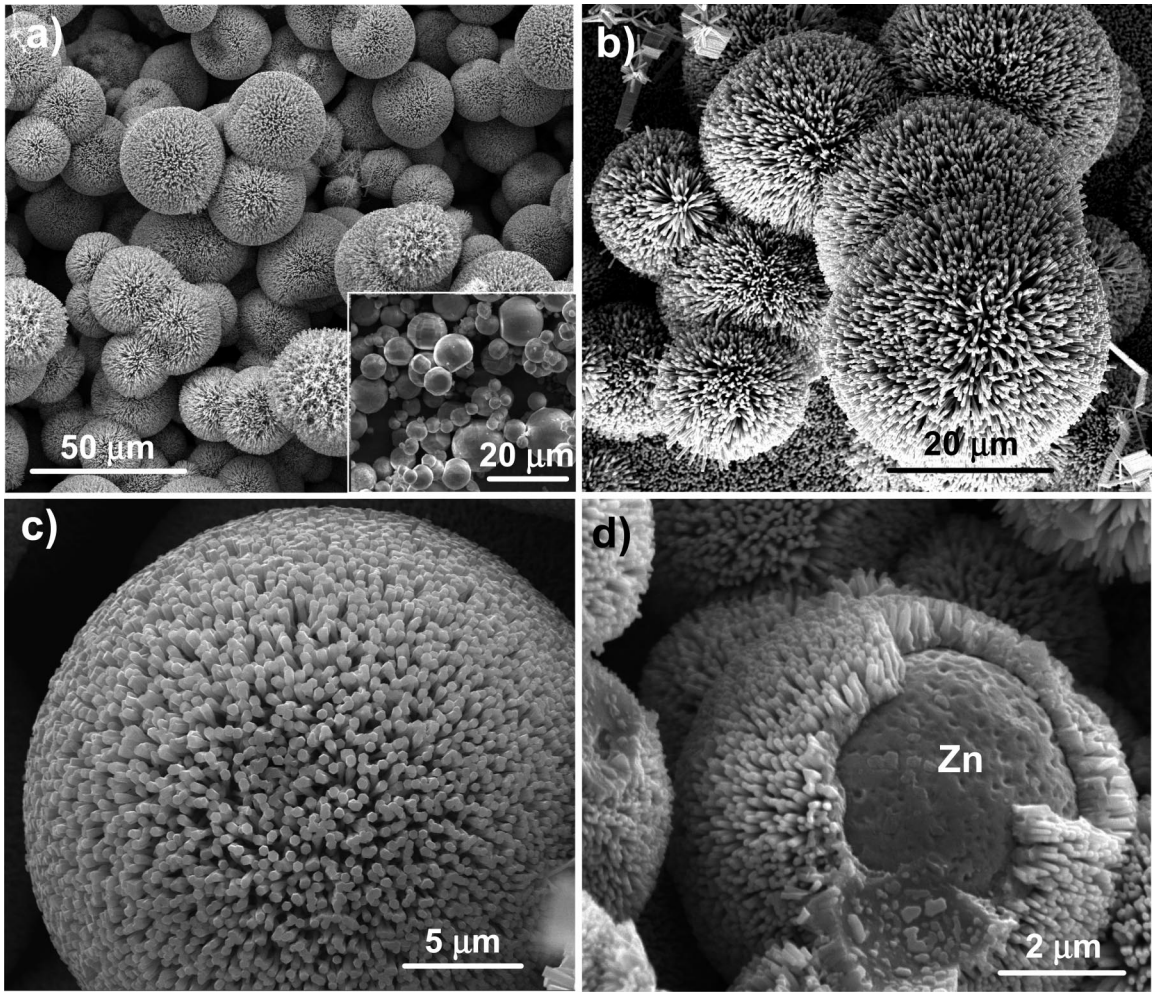

Figure 5. SEM images of urchin-like ZnO nanorod balls grown on zinc microspheres. (a) Low-magnification SEM image of ZnO nanorod balls. The inset shows the initial zinc microspheres. (b) High-magnification SEM image of several balls showing each ball is covered with dense ZnO nanorods growing along the ball's surface normal. (c) One 25-μm-diameter ZnO nanorod ball. (d) A broken ZnO nanorod ball showing ZnO nanorods growing along zinc core's surface normal.

point the surface of the zinc foil (or zinc balls) was in the melting state and thus can be immediately oxidized by oxygen to form a thin layer (~1 μm thick) of dense ZnO nanopillars (Figure 2). Like the ZnO nanocrystal seeds used in solution method,[17] the ZnO nanopillars formed at this initial growth stage are believed to act as the seeds for subsequent nanorod growth. This assumption was verified by the following two facts. (i) When silicon wafers or alumina plates were used as the substrates, only random ZnO nanorods were deposited on the substrate surfaces (in an recent report by Shen et al.[23] quasi-aligned ZnO nanonails and nanopencils were grown on silicon wafer surface by heating zinc powder at 600−700 °C in a tube furnace system, where the oxygen was probably from the system leaking). (ii) When no external zinc source was provided, the thickness of the ZnO nanopillars kept at ~1 μm regardless of the growth time. The later fact also indicates that the ZnO nanocrystal thin layer is seamlessly formed and firmly attached to the zinc foil surface, which protects inner zinc from being evaporated and oxidized during the nanorod growth process. Indeed, when the foil is intentionally broken after 10−30 min growth, unreacted metal zinc layer can be easily seen.

After the growth, the surface of the 10 cm × 1 cm zinc foil was covered with a thin white-gray layer. X-ray diffraction (XRD) analysis (Figure 3) shows that the deposit is wurtzite (hexagonal)-structured ZnO with lattice constants of $a = 3.249$ and $c = 5.206$ Å (JCPDS card No. 35-1451). The strong intensity of the (002) peak indicates that the ZnO structure has a preferential growth direction along the *c*-axis orientation.

Scanning electron microscopy (SEM) observations reveal that the entire substrate surface is covered with dense, highly aligned ZnO nanorods with growth direction perpendicular to the substrate surface (Figures 4). Because of the differences in temperature (from 500 ° to 450 °C) and oxygen concentration (from low to high) from the left end to the right end of the zinc foil, the morphologies and sizes of the as-synthesized ZnO nanorods across the 10 cm long foil vary gradually. Although there is no apparent boundary between adja-

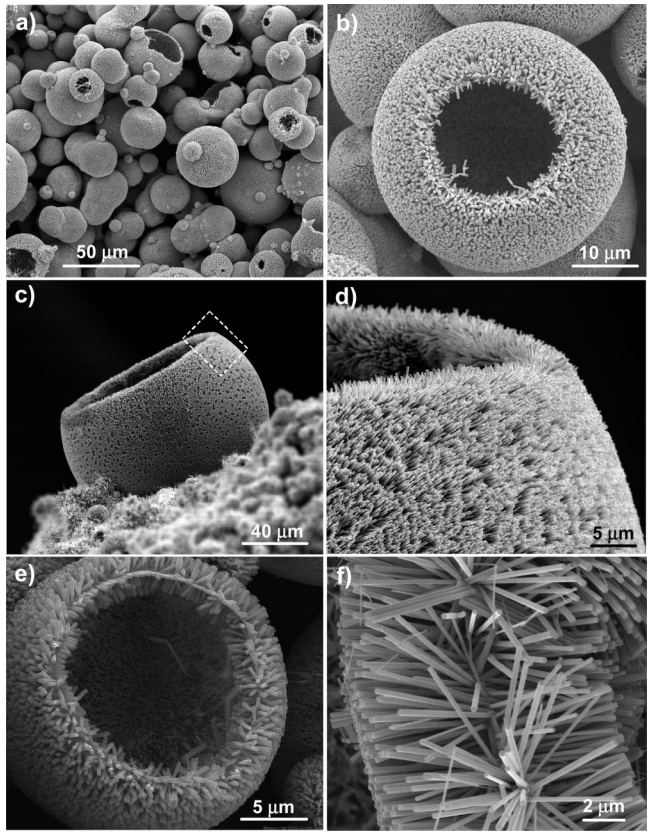

Figure 6. SEM images of urchin-like hollow ZnO nanorod bowls. (a) Low-magnification SEM image showing the presence of hollow ZnO nanorod bowls. (b) High-magnification SEM image of one 40-μm-diameter ZnO nanorod bowl. (c) One 130-μm-diameter ZnO nanorod bowl. (d) High-magnification SEM image of the boxed area in panel c, showing the surface of the bowl is covered with high density, uniform ZnO nanorods. (e) SEM image of one 25-μm-diameter ZnO nanorod bowl. The nanorods were grown on both the outer and inner surfaces of the bowl. (f) High-magnification SEM image of the edge area of a ZnO nanorod bowl showing dense, same size ZnO nanorods growing from both the outer surface and inner surface.

cent regions, four distinctive deposition zones can be identified on the basis of the morphologies and sizes of the nanorods, as that labeled in Figure 4a. From the left end to the right end, the morphologies of the products change from nanoneedles (zone 1; Figure 4b), to uniform nanorods (zone 2; Figure 4c,d), nanonails (zone 3; Figure 4e), and finally micronails (zone 4; Figure 4f,g). While the lengths of the nanorods formed in different zones are almost the same (~5 μm), the average diameters of the nanorods increase significantly from about 50 nm of the nanoneedles (Figure 4b) to about 200 nm of the uniform nanorods (Figure 4d) and nanonails (Figure 4e), and to about 500 nm of the micronails (Figure 4f,g; the diameters of the nail caps are up to 1 μm). Even though the growth temperature has some influence on the diameters of the nanorods, the major contribution is believed to come from the difference in oxygen concentration and thus the difference in ZnO reactant vapor concentration. Since the growth was conducted under 500 Torr of flowing argon gas and the outlet of the oxygen tube is located right above the boundary of zone 2 and zone 3, the oxygen concentration (and thus the ZnO reactant vapor concentration) over zone 3 and zone 4 should be much higher than that over zone 2 and zone 1 (due to back diffusion), resulting in the formation of larger and nail-like nanorods at the downstream region.[23]

The cross-sectional image of the nanorod array shown in Figure 4c reveals that the aligned ZnO nanorods grow perpendicularly from a ZnO thin film. Close observation (Figure 4d) clearly shows that the film is composed of dense ZnO nanocrystals and that the growth of ZnO nanorods was initiated from these nanocrystals. This observation confirms our assumption on the seeding function[17] of the nanocrystals. The top view images of the aligned ZnO nanorods (inset in Figure 4c, and Figure 4g) display perfect hexagonal cross section, indicating the preferential <0001> growth direction of the nanorods, which is in good agreement with the XRD result (Figure 3).

Besides the growth on flat zinc foils, our low-temperature oxidization method can also be used to grow dense ZnO nanorods on highly curved zinc surface. By replacing zinc foils with zinc microspheres and keeping the growth conditions unchanged, we were able to grow sophisticated urchin-like ZnO nanorod superstructures. Like the growth on zinc foils, the morphologies and sizes of the ZnO nanorods grown on zinc microspheres vary with the deposition regions. Accordingly, spherical ZnO assemblies based on ZnO nanoneedles, nanorods, nanonails, and micronails can be readily obtained. Figure 5a is a typical low-magnification SEM image of urchin-like ZnO nanorod balls formed in zone 2 position. The sizes of the nanorod balls vary from several micrometers to up to 100 micrometers, which are determined by the sizes of the original zinc microspheres (inset in Figure 5a). High-magnification SEM observations (Figure 5b,c) show that each ball is uniformly covered with dense, same length ZnO nanorods, forming a unique urchin-like nanorod superstructure. The ZnO nanorods always grow along the ball's surface normal regardless of the curvature of the zinc microspheres (Figure 5d).

While majority of the ZnO nanorod balls are in spherical shape and seemingly have a solid zinc core, bowl-like ZnO nanorod superstructures can be frequently obtained (Figure 6a), especially for samples after longer time (30 min) growth. These hollow balls still exhibit perfect spherical shape and can be regarded as a truncated hollow ball. High-magnification SEM observations (Figure 6b,c) show that ZnO nanorods were grown not only on the outer surface with growth direction along the ball's surface normal, but also on the inner surface with growth direction toward the ball center. The nanorods grown on both surfaces of the bowls have almost the same diameter, length, and density (Figure 6e,f). This unique growth phenomenon can be understood as follows. At the initial growth stage, ZnO

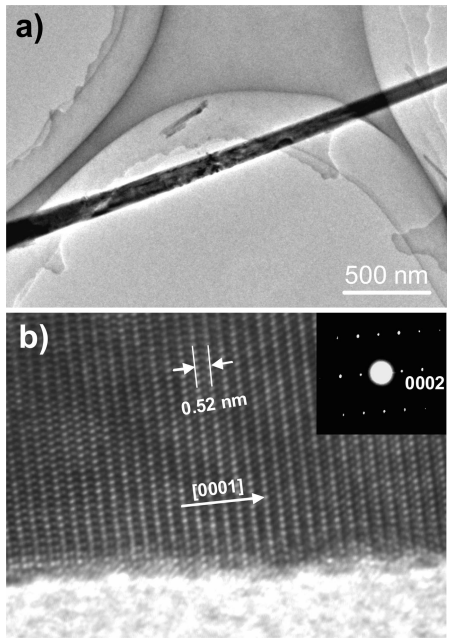

Figure 7. TEM images of ZnO nanorods: (a) low-magnification TEM image of a ZnO nanorod; (b) high-resolution TEM image of the edge part of a ZnO nanorod. The inset is the corresponding electron diffraction pattern.

nanocrystals are formed on the zinc sphere surface, forming a dense ZnO nanocrystals shell around the yet melted zinc core. These nanocrystals act as the seeds for subsequent nanorods growth by absorbing ZnO reactants from the vapor. Because the temperature (450−500 °C) at the deposition region is higher than zinc's melting temperature (419.5 °C), the zinc core will eventually be melted and zinc vapor will be generated inside the shell. If the shell is very dense and seamless, the inside zinc vapor pressure will be high enough that some shells will be broken and zinc will be evaporated. Because of the presence of oxygen in the vapor, the oxygen will diffuse into the cavity and react with zinc vapor to form ZnO reactant vapor that feeds the growth of ZnO nanorods on the shell's inner surface. Like the nanorods grown on the outer surface, the nanorods grown on the inner surface are also seeded by the ZnO nanocrystals.

The morphology and microstructures of the ZnO nanorods were further studied by transmission electron microscopy (TEM). Figure 7a is a TEM image of a ZnO nanorod. Even thought the present ZnO nanorods were grown at a much lower temperature than the previous high-temperature processes,[5,6,20−22] high-resolution TEM (Figure 7b) and selected area electron diffraction (inset in Figure 7b) studies reveal that the nanorods are single-crystalline with growth direction along <0001>. The surface of the nanorod is clean, atomically sharp, and without any amorphous sheathed phase.

The photoluminescence (PL) spectra of the aligned ZnO nanorods were measured by using a

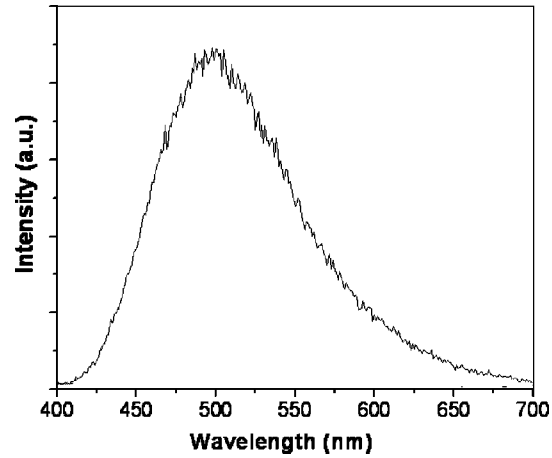

Figure 8. Photoluminescence spectrum of ZnO nanorods showing a strong, broad green emission peaking at about 500 nm.

Xe lamp (325 nm) as the excitation source. Figure 8 shows a room-temperature PL spectrum recorded from ZnO nanorods grown on zinc foil. A strong, broad green emission peaking at ~500 nm was detected. The green emission from ZnO is commonly referred to as deep-level or trap-state emission,[24] which is generally attributed to singly ionized oxygen vacancies,[25] zinc vacancies and zinc interstitials,[26] or extrinsic impurities.[27,28] Since our ZnO nanorods were synthesized under the presence of excess oxygen, Zn vacancies may be responsible for the green emission.

CONCLUSIONS

In summary, we have demonstrated a catalyst-free, low-temperature oxidization method to large-scale growth of vertically aligned ZnO nanorod arrays on zinc foils. The control of oxygen introduction and the formation of ZnO nanocrystals on the zinc foil surfaces at the early growth stage play critical roles on the success of the synthesis. Besides the growth on conductive zinc foils, this method may also be applied to other substrates (such as silicon wafer, sapphire, graphite, metals, etc.) by electron-beam deposition (or thermal evaporation) of a zinc thin layer on the related substrates. By replacing zinc foils with highly curved zinc microspheres, unique urchin-like ZnO nanorod superstructures were readily obtained. The as-synthesized two-dimensional ZnO nanorod arrays formed on zinc foils and the three-dimensional urchin-like ZnO nanorod superstructures formed on zinc microspheres offer great opportunities for investigating the effects of spatial orientation and arrangement of one-dimensional nanorod building blocks on their collective sensing, optical, electronic, and optoelectronic properties.

METHODS

The growth was conducted inside a tube furnace system (Figure 1). Zinc powder was used as the source material and zinc foils or zinc microspheres were used as the growth substrates. In a typical run with a zinc foil as the substrate, ~0.5 g zinc powder was placed in an alumina boat which was then inserted at the center of an alumina tube, where the temperature is set at 600 °C. A piece of zinc foil (10 cm long, 1 cm wide, and 0.5 mm thick) was placed at downstream part of the alumina tube where the temperature is at ~450−500 °C, right above the melting temperature of zinc (419.5 °C). Argon (flow rate: 100 sccm) was used as the carrier gas to transport zinc vapor to the growth zone, where the zinc vapor meets and reacts with oxygen (flow rate: 3−5 sccm) to form ZnO vapor species to feed the ZnO nanorod growth. The pressure of the tube was held at 500 Torr and the growth time varied from 10 to 30 min.

For the growth using zinc microspheres as the substrates, the zinc microspheres were deposited on a long alumina supporting substrate (~10 cm long and 1.5 cm wide) by evaporating zinc powder at 600 °C under 200 Torr, 100 sccm of flowing argon for 15 min. The sizes of the zinc microspheres vary from several micrometers to tens of micrometers (see the inset in Figure 5a). The subsequent nanorod growth procedure keeps the same as the growth on zinc foils.

The morphology of the ZnO nanorods were characterized by a FEI Inspect F field emission gun SEM operating at 15 kV. The microstructure was investigated with a Hitachi HF-2000 TEM operating at 200 kV. The crystal structures were measured by a PANalytical X'Pert PRO X-ray diffractometer with Cu Kα radiation. The photoluminescence properties were studied with a Horiba Jobin Yvon FluoroLog3−2iHR320 spectrofluorometer using a Xe lamp as the excitation source. The excitation wavelength was 325 nm.

Acknowledgment. This work was supported by the University of Georgia Research Foundation, the US Office of Naval Research (under contract No. N004315578), and the Oak Ridge National Laboratory (ORNL) through the support from the U.S. Department of Energy, Office of Basic Energy Sciences (BES)—Division of Materials Sciences and Engineering (DMSE). ORNL is managed by UT-Battelle, LLC, for the US Department of Energy (DOE) under contract No. DE-AC05-00OR22725.

REFERENCES AND NOTES

1. Özgür, Ü.; Alivov, Ya. I.; Liu, C.; Teke, A.; Reshchikov, M. A.; Dogan, S.; Avrutin, V. S.; Cho, S. J.; Morkoç, H. A Comprehensive Review of ZnO Materials and Devices. *Appl. Phys. Rev.* **2005**, *98*, 041301.
2. Pearton, S. J.; Norton, D. P.; Ip, K.; Heo, Y. W.; Steiner, T. Recent Progress in Processing and Properties of ZnO. *Prog. Mater. Sci.* **2005**, *50*, 293–340.
3. Look, D. C.; Claflin, B.; Alivov, Y. I.; Park, S. J. The Future of ZnO Light Emitters. *Phys. Stat. Sol. A* **2004**, *201*, 2203–2212.
4. Service, R. F. Will UV Lasers Beat the Blue. *Science* **1997**, *276*, 895.
5. Pan, Z. W.; Dai, Z. R.; Wang, Z. L. Nanobelts of Semiconducting Oxides. *Science* **2001**, *291*, 1947–1949.
6. Huang, M. H.; Mao, S.; Feick, H.; Yan, H. Q.; Wu, Y. Y.; Kind, H.; Weber, E.; Russo, R.; Yang, P. D. Room-Temperature Ultraviolet Nanowire Nanolasers. *Science* **2001**, *292*, 1897–1899.
7. Park, W. I.; Yi, G. C. Electroluminescence in *n*-ZnO Nanorod Arrays Vertically Grown on *p*-GaN. *Adv. Mater.* **2004**, *16*, 87–90.
8. Law, M.; Greene, L. E.; Johnson, J. C.; Saykally, R.; Yang, P. D. Nanowire Dye-Sensitized Solar Cells. *Nat. Mater.* **2005**, *4*, 455–459.
9. Park, W. I.; Kim, J. S.; Yi, G.; Lee, H. J. ZnO Nanorod Logic Circuits. *Adv. Mater.* **2005**, *17*, 1393–1397.
10. Wagner, R. S.; Ellis, W. C. Vapor-Liquid-Solid Mechanism of Single Crystal Growth. *Appl. Phys. Lett.* **1964**, *4*, 89–90.
11. Ng, H. T.; Li, J.; Smith, M. K.; Nguyen, P.; Cassell, A.; Han, J.; Meyyappan, M. Growth of Epitaxial Nanowires at the Junctions of Nanowalls. *Science* **2003**, *300*, 1249.
12. Yan, M.; Zhang, H. T.; Widjaja, E. J.; Chang, R. P. H. Self-Assembly of Well-Aligned Gallium-Doped Zinc Oxide Nanorods. *J. Appl. Phys.* **2003**, *94*, 5240–5246.
13. Park, W. I.; Kim, D. H.; Jung, S. W.; Yi, G. C. Metalorganic Vapor-Phase Epitaxial Growth of Vertically Well-Aligned ZnO Nanorods. *Appl. Phys. Lett.* **2002**, *80*, 4232–4234.
14. Wu, J. J.; Liu, S. C. Low-Temperature Growth of Well-Aligned ZnO Nanorods by Chemical Vapor Deposition. *Adv. Mater.* **2002**, *14*, 215–218.
15. Yuan, H.; Zhang, Y. Preparation of Well-Aligned ZnO Whiskers on Glass Substrate by Atmospheric MOCVD. *J. Cryst. Growth* **2004**, *263*, 119–124.
16. Vayssieres, L. Growth of Arrayed Nanorods and Nanowires of ZnO from Aqueous Solutions. *Adv. Mater.* **2003**, *15*, 464–466.
17. Greene, L. E.; Law, M.; Goldberger, J.; Kim, F.; Johnson, J.; Zhang, Y.; Saykally, R.; Yang, P. D. Low-Temperature Wafer-Scale Production of ZnO Nanowire Arrays. *Angew. Chem., Int. Ed.* **2003**, *42*, 3031–3034.
18. Greene, L. E.; Law, M.; Tan, D. H.; Montano, M.; Golderger, J.; Somorjai, G.; Yang, P. D. General Route to Vertical ZnO Nanowire Arrays Using Textured ZnO Seeds. *Nano Lett.* **2005**, *5*, 1231–1236.
19. Tian, Z. R.; Voigt, J. A.; Liu, J.; McKenzie, B.; McDermott, M. J.; Rodrigue, M. A.; Konishi, H.; Xu, H. Complex and Oriented ZnO Nanostructures. *Nat. Mater.* **2003**, *2*, 821–826.
20. Yan, H. Q.; He, R. R.; Pham, J.; Yang, P. D. Morphogenesis of One-Dimensional ZnO Nano- and Microcrystals. *Adv. Mater.* **2003**, *15*, 402–405.
21. Yan, H. Q.; He, R. R.; Johnson, J.; Law, M.; Saykally, R. J.; Yang, P. D. Dendritic Nanowire Ultraviolet Laser Array. *J. Am. Chem. Soc.* **2003**, *125*, 4728–4729.
22. Pan, Z. W.; Mahurin, S. M.; Dai, S.; Lowndes, H. L. Nanowire Array Grating with ZnO Combs. *Nano Lett.* **2005**, *4*, 723–727.
23. Shen, G. Z.; Bando, Y.; Liu, B. D.; Golberg, D.; Lee, C. J. Characterization and Field-Emission Properties of Vertically Aligned ZnO Nanonails and Nanopencils Fabricated by a Modified Thermal-Evaporation Process. *Adv. Funct. Mater.* **2006**, *16*, 410–416.
24. Huang, M. H.; Wu, Y. Y.; Feick, H.; Tran, N.; Weber, E.; Yang, P. D. Catalytic Growth of Zinc Oxide Nanowires by Vapor Transport. *Adv. Mater.* **2001**, *13*, 113–116.
25. Vanheusden, K.; Warren, W. L.; Seager, C. H.; Tallant, D. R.; Voit, J. A.; Gnade, B. E. Mechanisms Behind Green Photoluminescence in ZnO Phosphor Powders. *J. Appl. Phys.* **1996**, *79*, 7983–7990.
26. Bylander, E. J. Surface Effects on the Low-Energy Cathodoluminescence of Zinc Oxide. *J. Appl. Phys.* **1978**, *49*, 1188–1195.
27. Dingle, R. Luminescent Transitions Associated With Divalent Copper Impurities and the Green Emission from Semiconducting Zinc Oxide. *Phys. Rev. Lett.* **1969**, *23*, 579–581.
28. Garces, N. Y.; Wang, L.; Bai, L.; Giles, N. G.; Halliburtin, L. E.; Cantwell, G. Role of Copper in the Green Luminescence from ZnO Crystals. *Appl. Phys. Lett.* **2002**, *81*, 622–624.